Corona Charging and Current Measurement using Phi-type Corona Electrodes

T. Sugimoto, H. Ishii, and Y. Higashiyama, *Member, IEEE*

Abstract — **In order to develop a non-contact surface resistivity measurement, corona charging of a test material under simultaneously measurement of a surface potential or an induction current caused by the traveling surface charge have been investigated using phi-type electrodes. The phi-type electrode consisted of a high voltage needle electrode that penetrates a circular hole of a grounded planar electrode. The phi-type electrode was positioned over electrically isolated test materials. The purpose of the design was to supply static charges on the test surface, to give a ground potential above the charged test material, and to measure the surface potential or the induction current caused by the propagated surface charge. The test materials with the surface resistivities of 10^6 to 10^{12} Ω were prepared by coating conductive polymer layers on the PVC disk. Two kinds of setup were prepared for higher surface resistivity (Model H) and lower surface resistivity (Model L). The Model H had a surface voltmeter to measure the slow propagation of surface charge. The rise time of the surface potential was linearly increased with the surface resistivity of 3 x 10^9 to 3 x 10^{12} Ω. The Model L had two induction probes to measure the fast propagation of the surface charge. The rate of total induction charges was a function of the surface resistivity of 3 x 10^6 to 3 x 10^9 Ω. The phi-type electrodes was found to be effective for non contact surface charge measurement of dissipative materials.**

***Index Terms*— Surface resistivity, Charge decay, Corona discharge, Electric field measurement, Induction current**

I. Introduction

Surface resistivity and charge decay measurement have been the ways to understand electrostatic properties of materials. For thick and solid materials except highly insulative materials, the surface resistivity measurement is preferably adopted rather than the charge decay measurement. As in IEC 60093 [1], two concentric electrodes are applied to a test surface where the leakage current flowing through the two electrodes is measured. The surface resistivities are categorized into three groups, conductive (< 10^5 Ω), dissipative (between 10^5 and 10^{12} Ω), and insulative (>10^{12} Ω), depending on its electrostatic behavior [2].

On the other hand, for materials such as thin films, powders, particles or coatings, it is difficult to measure the surface resistivity. A contact of the electrodes and its leakage current measurement can cause measurement errors. In this case, the charge decay measurement using a corona charging should be adopted because there is no physical contact of electrodes to the materials. The surface potential decay for the test material is measured followed by a corona charging of the test surface. The measured charge decay time shows how quickly the static charge on the test dissipate through the surface. However, it is difficult to predict the surface resistivity from the measured charge decay time [3]. The difficulty comes from the way to charge up the test material and to measure the surface potential.

Typical corona charge decay equipment includes corona electrode to charge up the test material and an electrostatic voltmeter to measure the surface potential. The corona electrode and the surface voltmeter are normally separated. After the corona charging, the charged test material set on the rotating ground table is quickly transferred under an electrostatic voltmeter [4,5]. This method is effective only for insulative material having the decay time in the order of a second or more, because there is a measurement dead time to transfer the charged test material from the charging part to the measurement part. For a dissipative material, the surface charge rapidly dissipates after the charging before measuring the surface potential.

Chubb produced charge decay unit with a fast response electrostatic field meter [6]. JCI 155v5 Charge Decay Unit deposits a consistent amount of positive or negative charge onto the surface of the material by corona needle points. The samples are mounted between two conducting isolated plates. Once the charge is deposited onto the surface of the test material, the plate containing the corona points is retracted within 20 milliseconds and a field meter is exposed. The decay time can be measured from below 50 ms to many days. Dependence of charge decay characteristics on charging parameters were reported in [7] with both earthed backing and open backing measurement. There is no correlation between decay time and surface resistivity because of a capacitive loading effect [8].

The purpose of this study is to predict the surface resistivity of test materials from the surface potential measurement by improving corona charger [9]. It looks like the corona decay measurement, but the electrode arrangement is significantly different. To eliminate capacitive loading effect, a grounded potential is provided above the electrically isolated test materials by positioning a phi-type electrode. The phi-type electrode includes corona charger and electrostatic voltmeter to measure the surface potential. There is no moving part like as turn table or plates to transfer charged test material to the measurement part. The one dimensional simple model shows that the surface potential distribution and the rise time of the surface potential is found to be a function of surface resistivity.

This paper presents experimental study of the corona charging

and surface charge measurement using the phi-type electrode. Two kinds of experimental setup are prepared for higher and lower surface resistivity. Principles of these methods and experimental results are described.

II. Experimental setup

A. Phi-type electrodes

Fig. 1 (a) and (b) shows the corona charging electrodes referred to as phi-type electrodes Model H and Model L, respectively. Both electrodes have a needle electrode and a planar electrode. The planar electrodes have a circular hole of 4 mm in diameter where the needle electrode penetrates along the central axis of the hole, with a configuration similar to the Greek character "ϕ". The phi-type electrodes were positioned over the test material with a gap of 5 mm. A distance between a tip of the needle electrode and the planar electrode was 3 mm. The test material is electrically isolated from the ground. The grounded planar plate of the phi-type electrodes plays an important role for creating capacitive coupling to the test surface. A dc high voltage was applied to the needle electrode to emit corona ion from the tip. The surface of the test material was partly charged by the corona ions arrived at the surface close to the needle. The surface charge should propagate over the surface at a rate depending on the surface resistivity of the test material [9]. To detect the propagating surface charge, either surface potential or induction current was measured by the Model H or the Model L.

The Model H had a window on which the probe of the surface voltmeter (Shishido, Statiron DX) was mounted to measure the surface potential of the test surface as shown in Fig. 1 (a). The distance between the needle electrode and the probe was 29 mm. Preliminary the surface voltmeter was calibrated by applying known voltage to a conductive test surface. The response time of the surface voltmeter was approximately 800 ms.

For the test materials with low surface resistivity, the change in surface potential can be shorter than the response time of the surface voltmeter. Hence the induction current caused by propagating surface charge was measured by Model L shown in Fig. 1 (b). The grounded planar electrode included two detective areas of 6 x 24 mm, called detector A and B. These detectors were directly connected to a digital oscilloscope with an input impedance of 1 MΩ. The distances between the needle electrode and the center of the detector A or B were 9mm or 27.5 mm, respectively. By comparing the two induction current measured at the different position from the needle electrode, the propagation of the surface charge can be detected.

B. Test materials

Poly vinyl chloride (PVC) disks with a thickness of 1 mm and a diameter of 120 mm were prepared as test materials. A metal plate was also used as a conductive surface. These materials were placed on the insulator table.

The surface resistivity of pure PVC disk was over than 10^{13} Ω. By coating with a dissipative material layer, the surface resistivity of the disk was adjusted. Before coating the dissipative material, the surface of the disk was aged by ac corona discharge for 80 minutes to increase the wettability. The contact angle of water deposit reduced from 40 degree to 25 degree due to the ac corona discharge.

Ethanol solution of conductive polymer (Nagase, Denatoron P-502S) was coated on the surface of the test material by the spin coating method. The aged PVC disk was set on a rotating disk with a speed ranging from 800 to 6000 rpm. Droplets of 0.5 ml were repetitively dropped on to the center of the rotating PVC disk, creating thin layers on the

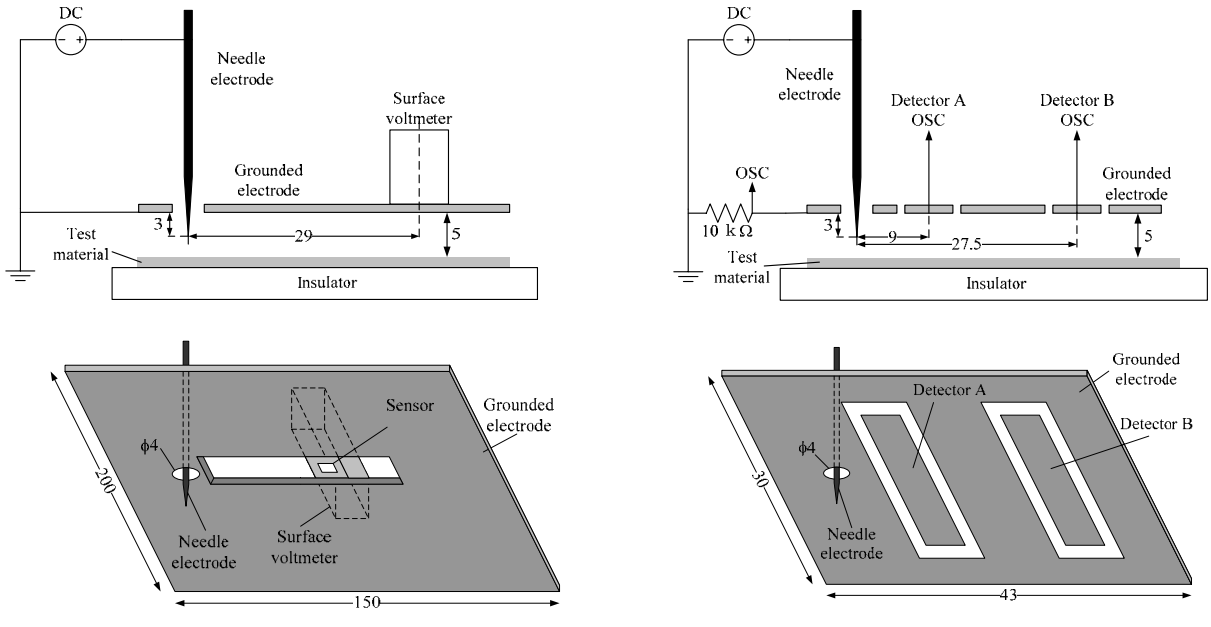

(a) Model H (b) Model L

Fig. 1 Phi-type electrodes Model H and Model L for non contact measurement of higher and lower surface resistivities.

surface of the disk. After the coating, the surface resistivity was measured by the surface resistivity meter (Trek Model 152). The surface resistivity could be widely adjusted ranging from 3 x 10^6 to 1 x 10^{12} Ω by the amount of droplets and the rotation rate.

C. Experiments

1) Surface potential measurement using the Model H

The rise time of the surface potential was measured by the Model H for test materials with various surface resistivities. The positive high voltage of + 3 kV was applied to the needle electrode at t=0. Time variation of the surface potential was measured by the electrostatic voltmeter. An output signal of the voltmeter was recorded by the digital oscilloscope (Yokogawa, DL6100). Because the test materials were electrically isolated from the ground, the surface potential was increased and eventually saturated at a certain values. The rise time of the surface potential was calculated from the time variation of the surface potential. The rise time was defined as the time when the surface potential becomes 0.9 E from an onset of corona charging, where E is the saturated value of the surface potential measured.

2) Current measurement using the Model L.

The induction currents caused by the traveling charge on the test surface were measured by two detecting electrodes A and B for various surface resistivities. In this experiment, the applied voltage to the needle electrode was slowly increased until the corona discharge onset to eliminate the induction current caused by rapid change in the applied voltage. The planar electrode except the detector A and B was also connected to the digital oscilloscope via 10 kΩ resistor to measure the corona discharge current. The induction current measurement of the detector A and B was triggered by the onset of the corona discharge. The measurement time was 200 μs after the corona onset. The sampling rate was 5MHz.

III. Results

A. Corona discharge current

The waveform of the corona discharge current at an onset voltage was measured for the Model L. Fig. 2 (a) and (b) show positive and negative corona discharge currents, respectively. For the positive corona, the corona onset voltage was + 2.1 kV. A pulse current with a peak value of 20 to 30 μA appeared as shown in Fig. 2 (a). There was no ion supply after the single corona pulse. Positive glow corona with no pulses was followed by the single corona pulse for higher applied voltages. On the other hand, two or three corona pulses with a peak value of – 10 to -15 μA appeared at a voltage of -1.6 kV for the negative corona as shown in Fig. 2 (b). The number of the corona pulses was increased with increasing the applied voltage. Trichel pulses were appeared at an applied voltage higher than - 3.2 kV.

In the positive corona, single and large pulse was appeared at the corona onset. This property was significantly important for detecting the traveling surface charge from the induction current, because the two waveforms of the induction currents measured at the detector A and B should be compared for a same corona pulse. For the negative corona, multiple pulses were appeared in the measurement time of 200 μs, resulting in the multiple and complex induction currents. In this experiments described below, positive corona was used for charging the test materials.

The property of the corona discharge for the Model H was almost the same as the Model L. When the dc high voltage of +3 kV was applied at t = 0 s, the positive glow corona was continuously occurred after the single corona pulse.

B. A rise time of surface potential

Fig. 3 shows examples of the applied voltage and the time variation of the surface potential for the Model H. As shown in Fig. 3 (a), the surface potential began to increase when the applied voltage became +2 kV where the positive corona discharge was onset. The increase in the surface potential should be caused by the continuous ion supply to the test material just below the needle electrode and the propagation of the surface charge to where the surface voltmeter was located. Because the test material was electrically isolated, the surface potential saturated when the surface was fully charged up. The positive glow corona discharge continued even when the surface potential saturated. In the steady state, the most of the corona ions directly traveled to the grounded planar electrode. For a surface resistivity of 1 x 10^{12} Ω, the surface potential slowly increased as shown in Fig. 3 (c) compared to the lower surface resistivity as in Fig. 3(a) or (b) caused by slower propagation of the surface charge.

Fig. 4 shows the time variations of normalized surface

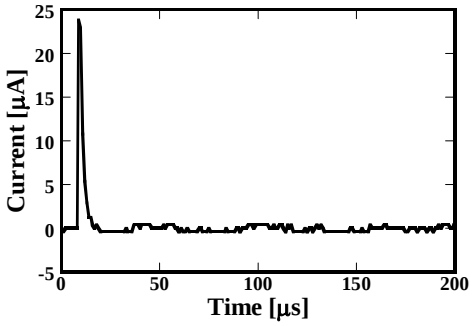

(a) Positive corona

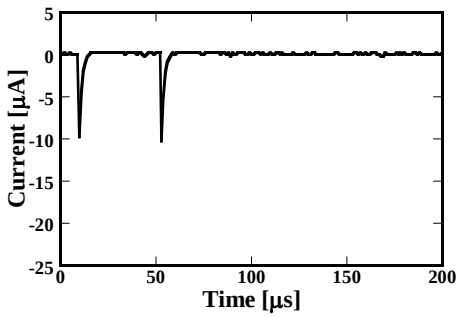

(b) Negative corona

Fig. 2. Waveforms of corona pulse at an onset voltage for positive and negative applied voltage.

potentials. The measured surface potential V was divided by its saturated value V_{MAX}. For the surface resistivities less than 10^9 Ω, the normalized surface potential took the same profile. The surface potential slowly increased with the surface resistivitis larger than 3 x 10^9 Ω. There was no potential increase for the surface resistivity over than 10^{13} Ω because the surface charge supplied to the surface remained at the area and never propagated over the surface.

Fig. 5 shows a relationship between the rise time of the surface potential and the surface resistivity. The rise time was approximately 800 ms for the surface resistivity lower than 3 x 10^9 Ω due to the response time of the surface volt meter. On the other hand, the rise time was linearly increased with the surface resistivities over than 3 x 10^9 Ω. The relationship shows that the surface resistivity ranging from 3 x 10^9 to 1 x 10^{12} Ω can be predicted from the rise time of the surface potential. The lower limit of the range was strictly confined by the response time of the surface volt meter used.

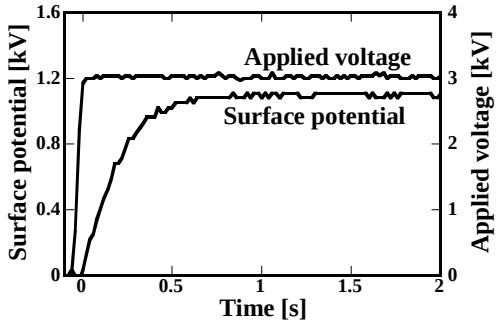

(a) 3 x 10^6 Ω

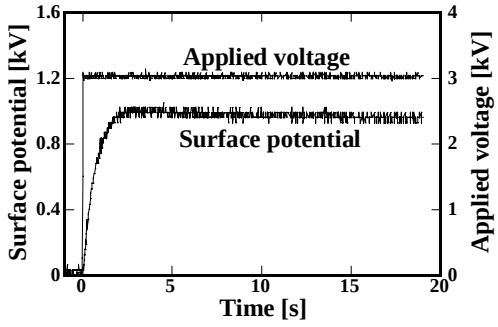

(b) 1 x 10^{11} Ω

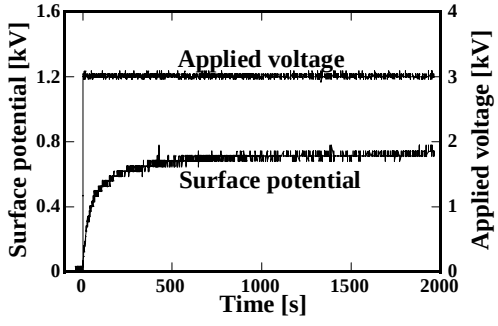

(c) 1 x 10^{12} Ω

Fig. 3. Time variations of the applied voltage and the surface potential for various surface resistivities.

C. *Induction current due to propagating surface charge*

Fig. 6 shows the induction currents flowing through detector A and B at a corona onset voltage for the Model L. In Fig. 6 (a), the metal plate was tested as a highly conductive surface. For the conductive metal surface, the profiles of the induction currents A and B were exactly the same as shown in Fig. 6 (a). Both induction currents A and B rapidly increased when the single corona pulse appeared and then gradually decreased. Just after the corona charging, the surface of the conducting material should have the same potential everywhere. Hence the induction currents A and B were also the same.

On the other hand, the induction current A and B significantly changed for the dissipative surface as shown in Fig. 6(b) to (f). In Fig. 6 (b), the induction current A rapidly increased at a corona onset while the induction current B slowly increased with a delayed peak of about 30 μs after the corona onset. It suggests that the surface charge slowly propagated compared to the conductive surface.

The peaks of the induction currents delayed for higher surface resistivities as shown in Fig. 6 (b) to (d). Also, the magnitude of the induction current B decreased with the surface resistivity. There was no difference in the induction current for the surface resistivity over than 10^9 Ω, as compared Fig. 6 (e) to Fig. 6 (f). The surface charge supplied by the single corona pulse might remain around the needle electrode in this time range. No traveling charge was observed. The small induction current appeared was due to the increase in the surface potential only around the needle electrode.

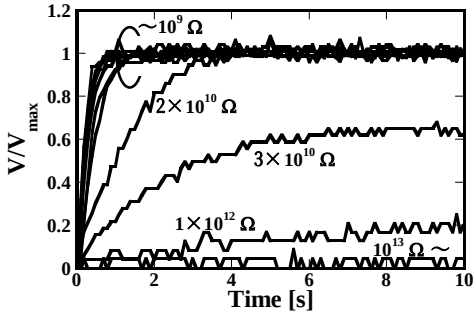

Fig. 4. Normalized surface potential for various surface resistivities.

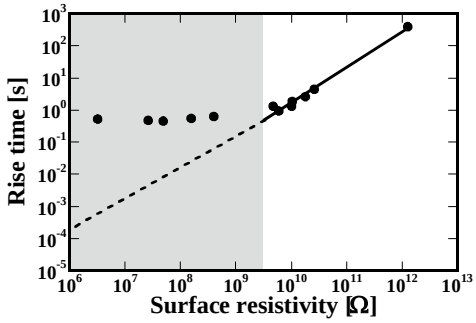

Fig.5. Relationship between the rise time and the surface reisitivities.

A charge amount calculated by the time integral of the induction current indicates the total induced in 180 μs. Here the total induction charge flowing to the detector A and B are defined as Q_A and Q_B. The rate Q_A/Q_B indicates some kind of mobility of surface charge on the test material. For the highly conductive surface the rate should be 1, because the charge densities of these two areas become the same value immediately after the corona charging as expected from Fig. 6 (a). If the propagation of the surface charge is suppressed by the surface resistivity, the surface charge density decreased with a distance from the needle electrode. Hence the rate of Q_A/Q_B will be larger than 1.

Fig. 7 shows the relationship between the surface resistivity and the rate Q_A/Q_B. The rate Q_A/Q_B for the surface resistivity of 3 x 10^6 Ω is still 1 regardless of the drastic change in the waveform of the induction current as shown in Fig. 6 (b). The rate varied from 1 to 7 with increasing the surface resistivity from 3 x 10^6 Ω to 3 x 10^9 Ω. For the surface resistivity over than 3 x 10^9 Ω the rate is constant because there is no traveling charge in this time range. The induction current measurement and the calculated rate of the traveling total charge measured at the different point was significantly sensitive in the lower surface resistivity less than 3 x 10^9 Ω.

IV. Discussion

Osawa shows analytical solutions of surface potential distribution on thin material with a grounded backing

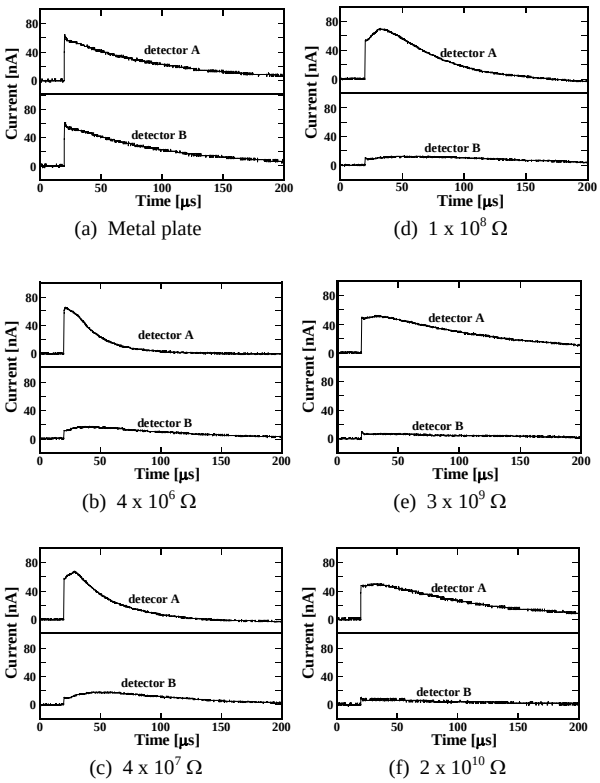

(a) Metal plate (d) 1 x 10^8 Ω

(b) 4 x 10^6 Ω (e) 3 x 10^9 Ω

(c) 4 x 10^7 Ω (f) 2 x 10^{10} Ω

Fig. 6. Induction current waveforms of detector A and B for various surface resistivities.

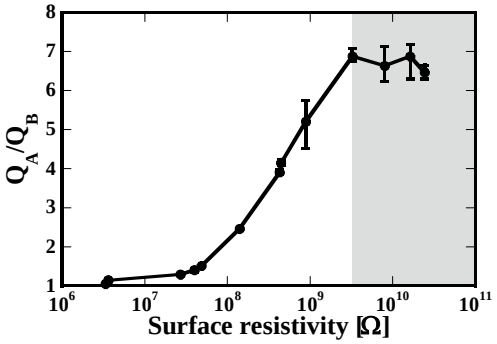

Fig. 7. Relationship between the surface resistivity and the rate of the time integral of the induction currents Q_A/Q_B.

conductor [10]. It was found that the surface potential distribution is a function of $\rho_s/\rho_v\delta$, that is, the ratio of surface resistance to volume resistance per unit area, where ρ_s: surface resistivity, ρ_v: volume resistivity, δ: thickness of the material. In this study, the grounded planar electrode was positioned above the test material which was isolated from the ground. If we suppose that the air gap as an insulator with a thickness of δ, the air can be regarded as a thin material with a grounded conductor in the top side and with a test surface in the bottom side. Hence the surface potential distribution can be a function of $\rho_s/\rho_v\delta$, where ρ_s: surface resistivity of test material, ρ_v: volume resistivity of air, δ: the gap of air. Because the volume resistivity of air and the air gap are constant values, the surface potential distribution of the test material can be a function of ρ_s. The potential distribution is also a function of time in the transient state. One dimensional model also show that the surface potential distribution and the rise time of the surface potential is a function of ρ_s and time [9].

From the theoretical point of view, the surface potential of the test surface eventually reach the same potential everywhere on the test surface because of the charge propagation over entire surface [9]. However, for the insulator surface with a resistivity over than 10^{13} Ω, there was no potential increase as shown in the experimental data of Fig. 4(c). The neutralization of the surface charge due to ions existing in air gap might be one of the possible reasons. No potential increase can even be a measure of surface resistivity, indicating the surface is highly insulative.

For the dissipative surface, there was linear relationship between the rise time of surface potential and the surface resistivity as shown in Fig. 5 for the Model H. The lower limit of the measurement derived from the dead time of the measurement due to the response time of the surface voltmeter. If the surface meter with faster response time can be used, the lower limit of the measurement can be extended. However, another approach to extend measuring range, that is, induction current measurement, could be verified for the lower surface resistivity.

The induction current of A and B could detect traveling charge for the surface resistivity less than 3 x 10^9 Ω. The rate of the total charge calculated by the time integral of the induction

current Q_A/Q_B is a function of the surface resistivity as shown in Fig. 7. Because the profiles of the induction currents of 3 x 10^6 Ω as in Fig.7(b) was significantly different from that of the conductive metal surface as in Fig. 7 (a), the lower limit of the measurement is expected to be extended by comparing the peak values of the induction current A to that of B.

If the surface resistivity measurements using the Model L and H are combined, the measuring range can be from 10^6 to 10^{12} Ω. It is significantly useful for assessing antistatic material because there is no physical contact on the test surface.

V. Conclusion

Corona charging and induction current measurement including surface potential measurement have been investigated for the sake of non contact surface resistivity measurement. The surface potential measurement using phi-type corona electrodes Model H can measure the surface resistivity from 3 x 10^9 to 1 x 10^{12} Ω. No potential increase was obtained for the insulative surface over than 10^{13} Ω. The induction current measurement can measure the lower surface resistivity from 3 x 10^6 to 3 x 10^9 Ω. Future works will include the combination of the surface potential measurement and induction current measurement to extend the measuring range.

VI. Acknowledgments

The authors wish to thank NAGASE & CO. LTD Japan for providing samples of conducting polymer. This study is supported by a Grant-in-Aid for Science Research No. 20560257 from the Ministry of Education, Culture, Sports, Science and Technology of Japan.

References

[1] International Standard 60093, 1980
[2] N. Jonassen, “Electrostatics”, p.56, Chapman & Hall, 1998
[3] G. Baumgartner: “ Electrostatic decay measurement theory and applications”, EOS/ESD symposium 95, pp. 262-272.
[4] For example, S. Sahli, A. Bellel, Z. Ziari, A. Kahlouche, Y. Segui :”Measure and analysis of potential decay in polypropylene films after negative corona charge deposition”, J. Electrostatics 57, (2003), pp. 169-181
[5] Japanese Industrial Standard L 1094, 1997
[6] J. N. Chubb: ”Instrumentation and standards for testing static control materials”, IEEE Trans. Ind. Appl 26 (6) Nov/Dec 1990, pp. 1182-1186
[7] International Standard 61340-2-1, Jul. 2002US
[8] J. N. Chubb: “Dependence of charge decay characteristics on charging parameters”, Electrostatics 1995, pp. 103-108.
[9] T. Sugimoto, H. Ishii, Y. Higashiyama: “Non-contacting measurement of surface resistivity using a phi type electrodes”, Proc. of IEEE Ind. Appl. Soc. Annural meeting, IAS32p1, 2008
[10] A. Osawa: “Theory of electrostatic characterization for thin materials with a grounded backing conductor”, J. Electrostatics Vol. 64, Issue 6, pp. 392-399, 2006